Jurnal Polimesin
Department of Mechanical Engineering
State Polytechnic of Lhokseumawe
http://e-jurnal.pnl.ac.id/polimesin
e-ISSN : 2549-1999 No. : 2 Month : April
p-ISSN : 1693-5462 Volume : 22 Year : 2024

Article Processing Dates: Received on 2024-02-16, Reviewed on 2024-03-11, Revised on 2024-03-23, Accepted on 2024-04-03 and Available online on 2024-04-30

Rotary friction welding of 304 stainless steel: parametric study, mechanical properties, and microstructure of the joint

Hudiyo Firmanto[1*], Susila Candra[1], Mochammad Arbi Hadiyat[2]
[1]Department of Mechanical and Manufacturing Engineering, University of Surabaya, Surabaya, 60292, Indonesia
[2]Department of Industrial Engineering, University of Surabaya, Surabaya, 60292, Indonesia
*Corresponding author: hudiyo@staff.ubaya.ac.id

Abstract

In the rotary friction welding process, the selection of process parameters affects the friction, heat generation, and joint formation. These factors collectively cause microstructural changes that determine the mechanical properties of the joint. Therefore, the process parameters, microstructure, and mechanical properties were interconnected during rotary friction welding. This study examined the influence of process parameters on their correlation with microstructure and mechanical properties in the rotary friction welding of 304 SS. A 3×4 full factorial experimental design was used to evaluate the effects of the process parameters on the microstructure and strength of 304 SS joints produced through rotary friction welding. An accurate evaluation of joint strength was performed using the notch tensile test technique. The joint with the highest strength was achieved by applying a combination of friction pressure and friction time at 55 bars and 3 seconds, respectively, resulting in a welding efficiency of 103.6%. A very low friction time (i.e., 5 s) produced a weak joint, which should be avoided. The welding process created three distinct structural zones in the joint: a joint structure finer than the parent metal structure, a partially deformed structure, and a heat-affected zone with deformation. Hardness tests of the joints showed a high hardness in the deformed structure. The formed structure contributes to the resulting joint strength.

Keywords:
Rotary friction welding, AISI 304, factorial, design of experiment, microstructure, tensile strength.

1 Introduction

Austenitic stainless steel is commonly used in various industries due to its high corrosion resistance, good strength, and formability. Stainless steel 304 typically contains 18% chromium and 8% nickel, as well as the highest carbon content of 0.08%. The addition of nickel helps to create an austenitic structure, improving ductility and corrosion resistance. Similarly, the addition of carbon enhances the mechanical properties[1].

The joining of 304 stainless steel is often required, and various welding methods have been used for this purpose, including liquid state (fusion welding) and solid-state welding (friction welding)[2]. The fusion welding technique has several advantages [3]. This process involves high temperatures that cause melting and solidification. Fusion welding in steel presents challenges due to the melting and solidification processes involved. Cooling from high temperatures can lead to phase transformations, resulting in the formation of intermetallic phases that compromise joint strength. This phenomenon is often attributed to the use of electrodes containing specific elements. Additionally, oxides may form in the welded area due to the reaction of molten metal with elements in the atmosphere.

The Rotary Friction Welding (RFW) method can be an alternative for welding stainless steel. RFW is a solid-state welding process used to join metals. In this technique, one material is rotated in relation to another while applying axial compressive pressure. RFW prevents the materials from melting during the welding process. The lower heat energy involved in RFW leads to shorter heating and cooling cycles, thereby reducing the likelihood of new phase formation. Additionally, RFW does not necessitate the use of filler metal, eliminating the introduction of new elements at the joint.

The RFW process has been used to join various materials. Many studies have also been conducted on joining metals using RFW. The joining of carbon steel using RFW was performed to study the mechanical properties of the joint [4], [5], [6]. Studies have also been performed on joining stainless steel [7], [8], [9], [10], [11], [12], non-ferrous metals, and dissimilar materials [13], [14], [15], [16], [17].

The friction of the surfaces of the materials generates heat, which plasticizes them. Heat power is primarily determined by friction torque and friction speed [7], [8]. Therefore, rotation speed, friction pressure, and forging pressure are crucial parameters for producing connections in metal RFW. Increasing any of these parameters increased the amount of heat produced during the heating stage. These parameters are associated with the structure generated at the joints and contribute to the strength of the connections. Several studies have been conducted on carbon steel joints [4], [5], [6]. In medium carbon steel joints, higher friction pressure resulted in increased joint strength. This strength was generated by a deformed structure with fine grains [4]. In low carbon steel joint research, rotation speed contributed the most to the strength [6]. The study also found that the strength of the joints is produced by fine grains in the connections.

Friction pressure enhanced the strength and hardness in the joint region of 304H stainless steel welded using RFW[7]. Equiaxed grains were observed in the joints. The study indicated that increasing friction pressure did not lead to grain growth, suggesting that the heat generated by friction is insufficient for such growth to occur. The energy required for the Rotary Friction Welding (RFW) process has been found to depend on the level of frictional pressure and rotational speed[8]. This study demonstrated that increasing forging pressure improves the tensile strength of the joints, but beyond a certain threshold, the strength increment diminishes. Dynamic recrystallization occurred in the welding zone, as indicated by the presence of equiaxed grains. Unlike the previous study, this research revealed that a greater energy input allows for grain growth, as evidenced by the larger growth at the joint. Therefore, all parameters, including friction pressure, rotational speed, and welding time, influenced the outcome of the joint by affecting the magnitude of input energy. Additionally, alongside friction pressure and forging pressure, welding time has been identified as the most influential factor in enhancing the strength of 304 stainless steel welds using the RFW method [9]. The deformation resulted in a structure that is plastically or partially deformed at the joint. Another study indicated that excessively high rotational speeds widened the welding zone, thus reducing the strength. Conversely, excessively low rotational speeds failed to provide adequate heat for the formation of a strong joint[10].

The literature review underscores the significance of optimizing welding parameters in order to achieve robust and high-quality welds. Previous studies have shown that increasing

the rotational speed enhanced the strength of weld joints when utilizing the rotary friction welding method to weld 304 stainless steel[10]. Nevertheless, excessively high rotational speeds can lead to a decrease in joint strength due to the excessive width of the heat-affected zone. Conversely, if the rotational speed was too low, the generated friction was inadequate to produce the necessary heat for proper joint formation. Additional research has indicated that augmenting the friction time and pressure enhances the strength of 304 stainless steel joints[11]. However, it should be noted that the joint strength decreased once it reached the maximum time and friction limit. With fixed process parameters, the highest strength was achieved through a combination of 9 s of friction time and 60 MPa of pressure.

It was observed that at high temperature, mechanical properties of 304 stainless steel decreased and followed by a relatively low ductility [1]. However, strengthening of stainless steel deformed at high temperatures has been observed in the thermomechanical treatment of stainless steel [18]. This was due to the decrease in grain size caused by dynamic recrystallization. The Hall-Petch type relationship was observed in the hot deformation of the stainless steel.It is relevant to relate hot deformation to the RFW process, as they both involve the same phenomenon.

Observations of the effect of the Rotary Friction Welding (RFW) process on the hardness of 304 stainless steel did not indicate significant changes in the hardness in the joint area[11]. This occurred because the 304 stainless steel was not hardenable. The microstructural changes that occurredwere also claimed not to demonstrate hardening effects.However, other observations [10]indicated an increase in the joint hardness (240 HV) compared to that of 304 stainless steel (210 HV). The researcher stated that this was due to the peak temperature occurring at the joint.Meanwhile, around the joint, structural changes have reduced the hardness of 304 stainless steel. Therefore, speculation regarding changes in the properties of stainless steel due to the RFW process may arise.

The precise welding process is crucial in ensuring the successful fusion of metals and avoiding potential defects or structural weaknesses in the joints. However, it is essential to bear in mind that each type of material and welding configuration may have distinct requirements. Therefore, further research and experiments on specific materials and conditions are necessary to develop more detailed guidelines for optimal welding parameters.

The effects of process parameters on the weldment strength of rotary friction-welded 304 stainless steel (SS) were investigated in this study. A factorial experiment was conducted to achieve this objective. This experimental design wasinfluencedby multiple factors, individuals, and interactions. Furthermore, this technique can account for the interactions between factors. The factorial design produces reliable results in a wide range of experiments [9], [19].Additionally, the joint's microstructure was investigated. An assessment was made of the microstructural alteration of the joint. Therelationshipbetween the mechanical characteristics and the microstructure of a joint was studied.

2 Research Method

2.1 Material

304 SS material was supplied to a bar with a diameter of 16 mm. The chemical composition of the materials is listed in Table 1. Prior to welding, the material was cut in the length of approximately 120 mm. The material surfaces were machined to obtain flat surfaces. This was required to obtain a perfect mating surface during welding.

Table 1. Chemical compositions of the 304 stainless-steel material

%C	%Si	%Mn	%P	%S	%Cr	%Ni
0.044	0.67	1.05	0.022	0.006	18.13	8.05

Prior to welding, the material was cut in the form shown in Fig. 1. The surfaces of the materials were machined to get flat surfaces. This was required to obtain a perfect mating surface during welding. The surface of the material was also cleaned from dirt, oil, or other substances that may interfere with the joining.

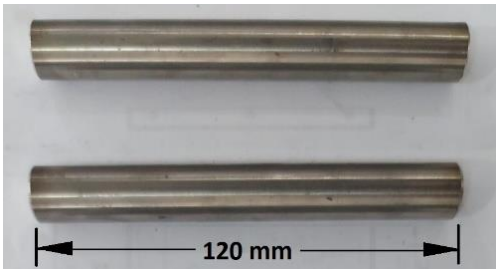

Fig. 1. Specimens for welding.

2.2 Equipment

Fig. 2 illustrates the RFW process. During this process, the surfaces of the two specimens werein contact. One specimen was held in a fixed chuck while the other was rotated. Axial pressure, also known as friction pressure, was applied to the specimen to create contact between surfaces. Once the set friction time was reached, the rotation of the spindle was stopped, and the forging pressure was applied to create axial contact pressure and complete the joining. After joining, excess material at the joint was removed using a turning machine. Subsequently, the sample was machined into a tensile test specimen.

The RFW experiments were conducted on a modified lathe machine[20]. The lathe machine, equipped with a hydraulic pack, is shown in Fig. 3. The spindle of the turning machine can hold and rotate the specimen at a specified speed determined by the gear box setting. A metal sleeve was fabricated and fixed to a machine slider to hold the specimen. A hydraulic power-pack unit was designed and installed to provide the necessary pressure for the welding process. The hydraulic unit was also equipped with a control system that allowed the user to set the pressure amount and duration. The design of the equipment allowed for the adjustment of various experimental parameters, such as spindle speed, friction, and forging pressure, as well as the friction and forging time. In each experimental trial, one specimen was securely attached to the spindle, whereas the other was affixed to the metal sleeve.

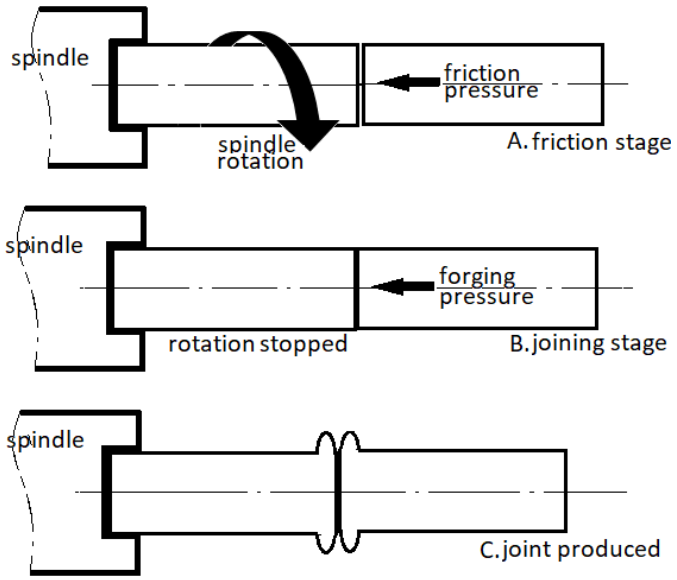

Fig. 2. Process of RFW.

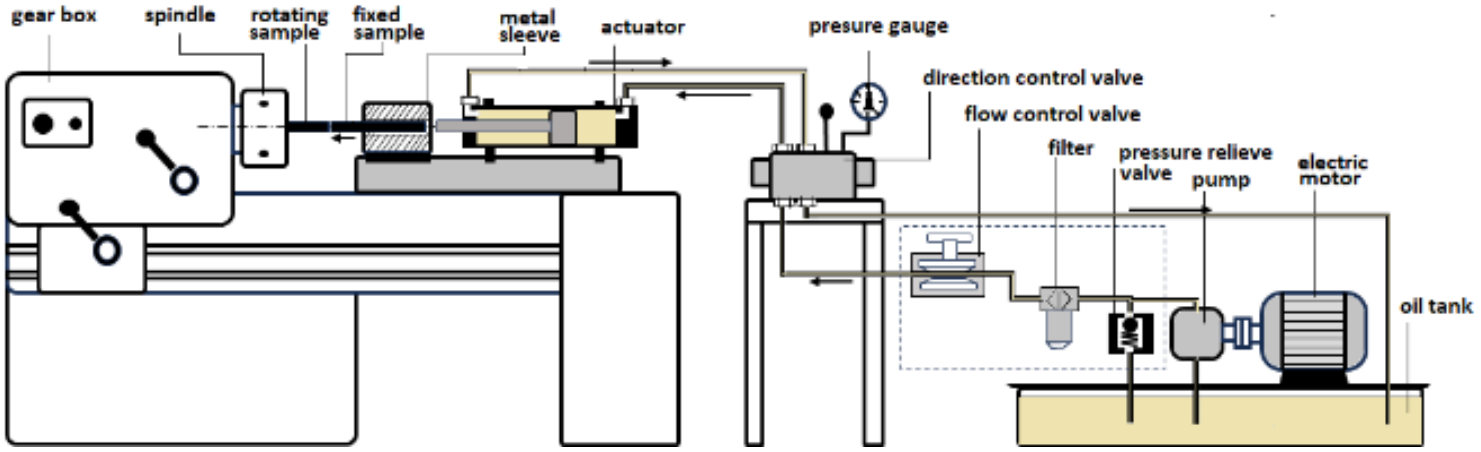

Fig. 3. The lathe machine was equipped with a hydraulic actuator and a hydraulic pack unit for the RFW process.

Prior to initiating the experiment, the surfaces of both specimens were carefully aligned. The spindle speed was selected based on the available speed provided by the machine. Pressure and time controllers were used to determine the duration and intensity of the applied pressure. Once the machine was activated, the specimen underwent rotation and was propelled by the hydraulic actuator's rod. This interaction established contact, resulting in the necessary friction and forging pressure on the surface of the specimen.

2.3 Design of Experiment

Exploratory experiments were carried out to determine factors and their levels. Previous studies indicated several factors that affect the RFW process, namely: friction time, friction pressure, spindle speed, and forging pressure and time [21], [22]. These parameters commonly alter the joint strength of metals in the RFW process. However, their roles vary according to the material used [13]. Therefore, it is necessary to examine the influence of these interactions. The present study aimed to investigate two factors related to the friction stage: friction pressure and friction time. The effects of individual factors and their interactions on the tensile strength of friction-welded 304 SS were investigated. The importance of individual factors on the joint strength of 304 SS has been reviewed [16]. The friction pressure and friction time were investigated individually by arranging the factor levels. This was intended to show the fluctuation of tensile strength while other factors were maintained constant. Hence, no interaction was involved. The possibility for these factors to interact was hinted at when joining different materials using RFW [22].

The present study examined the individual effects of friction pressure and friction time on Rotary Friction Welding (RFW) of 304 Stainless Steel (SS). Furthermore, an analysis was conducted to investigate their interactions that could significantly affect the tensile strength of the joint material. To accomplish this objective, the Design of Experiments (DoE) technique was employed. This approach was chosen to consider both individual and interaction effects, while also satisfying the statistical properties of DoE analysis.

Previous research has indicated that the recommended range for friction pressure in the friction welding of stainless steel and similar hard steels is between 15 and 90 bar, while the friction time should be between 5 and 30 s[11], [17]. These studies served as valuable references for determining the parameters for the main experiments. However, it should be noted that using bar units for pressure might imply hydraulic pressure. The actual interfacial pressure would depend on the construction of the hydraulic system, such as the diameter of the hydraulic piston used in the welding process. Therefore, in addition to consulting previous work, preliminary experiments were conducted to determine the appropriate levels of these factors. A series of RFW experiments were performed, starting from the lowest possible parameters and gradually increasing them until a joint could be produced. The lowest parameters that resulted in an appropriate joint, without generating any flash, were considered as the limit to be studied. Conversely, the highest parameters were associated with an acceptable level of flash. Beyond this limit, joints could still be obtained; however, excessive flash and axial length reduction would occur. This process led to the identification of the factors and their corresponding levels, as presented in Table 2.

After completing the level determination in Table 2, initial experiments were conducted to confirm that these are the suitable levels to get perfect joint friction welding. A friction pressure of five bars and a friction time of three seconds were selected to capture the critical level limit for welding the materials with an adequate joint. Accommodating these levels, a full factorial DoE was then chosen, and factors of interest were assigned within. Fixed factors with no variation were involved in this experiment and were excluded from the DoE design. For four levels of friction pressure and three levels of friction time, there were 12 treatments involved in the factorial DoE. To accommodate the interaction, a minimum of two replications were performed; hence, there were a total of 24 experimental runs in this design.

Table 2. Factor and level determination

Factors	Level 1	Level 2	Level 3	Level 4
Friction pressure (bar)	5	20	55	90
Friction time (seconds)	3	7	11	-
Forging pressure (bar)	Constant at 100			
Forging time (seconds)	Constant at 3			
Rotation speed (RPM)	Constant at 1330			
Response (MPa)	Joint tensile strength			

Tensile tests were performed according to ASTM E8M to assess the tensile strength of the joints. A Lead well LTC-20B CNC lathe was employed to transform the welded rods into tensile test specimens (shown in Fig. 4). The tensile tests were performed on a Gotech 100KN universal testing machine, which was operated in displacement control and had a crosshead speed of 5 mm/min.


Fig. 4. Tensile test specimen based on ASTM E8M standard.

For metallographic examination, the welded sample was cross-sectioned using a cross-sectioning grinding machine. The surface was ground and polished using alumina particles. The sample's surface was etched using the aqua regia reagent (15 mL of HCl and 5 mL of HNO_3). The joint microstructure was observed using an Amscope ME300TC-14M3 optical microscope. Hardnes tests across the joint was carried out using Mitutoyo Micro-Vickers Hardnes Testing Machine HM-210.

3 Results and Discussion

3.1 Visual Observation

Samples of the welding result are given in Fig.5. The figure illustrates that stainless steel gives acceptable joint and regular flash. In joining 304 SS, flash was produced less excessively in the joint even at high friction parameters. Fig.5 shows the joined metals with three different friction parameters. Fig.5(c) is the sample welded with the lowest parameters results (P_f = 5 bar,t_f = 3), it is marked with very little flash. Although the flash was minimized, however, the joint was perfect.

Higher friction parameters produced more flash as seen in Fig. 5(b) (P_f = 55 bar, t_f = 7 s). The flash in the joint increased with the highest friction parameter (Fig.5(c), P_f = 90 bar, t_f = 11 s). Referring to the length of the samples after the welding, the figure also explains that the higher heating parameters create more length of reduction of the sample (burn-off length).

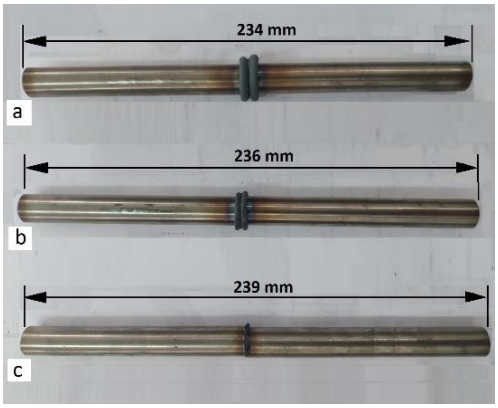

Fig. 5. Welded materials for tensile strength testing:(a) P_f = 90 bar, t_f = 11 seconds; (b) P_f = 55 bar, t_f = 7 seconds; (c) P_f = 5 bar, t_f = 3 seconds.

3.2 Microstructure of the Joint

The macrostructure of the 304 SS RFW joint is given in Fig.6. The figure shows a sound joint, and no crack or defect is formed. An interface layer is indicated at the joint and continues to form at the outermost part of the joint flash. Beyond the joint interface, two additional layers can be seen, namely: the Thermomechanically Affected (TMA) and Heat-Affected Zone (HAZ).

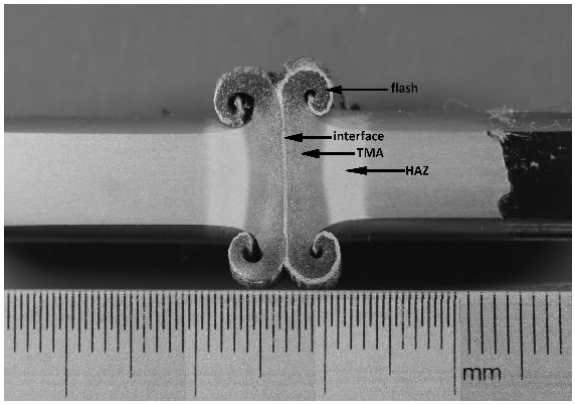

Fig. 6. Macrostructure of the 304 SS RFW joint.

The general microstructure of the joint is depicted in Fig.7. At the joint, three parts are indicated. An enlarged view of the structure is shown in the figure; therefore, it can be clearly seen. The three layers were more visible in the enlarged view of the general microstructure of the joint. An interface layer makes up the joint's structure. This layer was approximately 500 µm thick. A dark thin layer of approximately 200 µm was found near the interface. Beyond this layer, the microstructure was deformed, reaching the unaffected microstructure of the 304 stainless steel base metal.

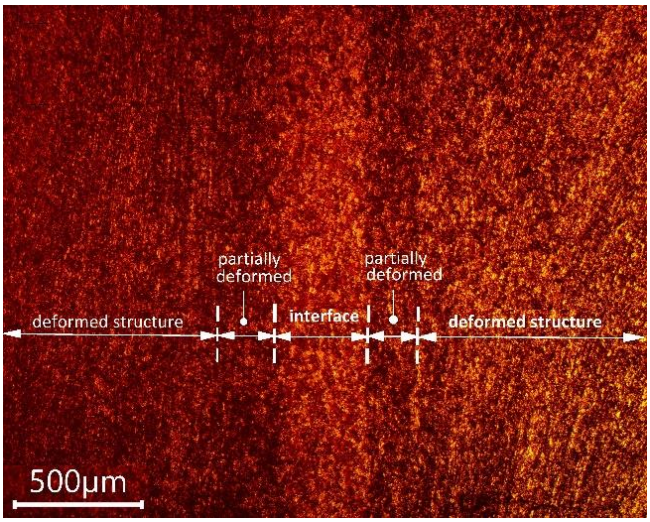

Fig. 7. General microstructure of the joint.

The microstructure revealed that perfect bonding was attained. It indicates the metallurgical bonding that produce the welding joint. In the RFW process, a welding joint was created owing to metallurgical bonding [23], [24], [25]. The temperature increased and constant application of pressure in the bonding interface for a determined time enables the atomic diffusion [23]. Excessive deformation allows the progress of the diffusion, and the centrifugal force due to the rotation of the specimen also influences the atomic diffusion at the interface [24], [25]. All of these factors are responsible for joint formation.

Since welding occurs in the solid state, defects in fusion welding of stainless steel (*e.g.*, arc or gas welding) due to melting conditions such as discontinuity [3] is rarely encountered in the RFW process. However, despite being known for producing good joints, the RFW process is not immune to the possibility of defects. Excessive flash formation, oxidation, and voids were found in joining titanium using the RFW technique[26]. Lack of bonding at the outermost circle was observed in welding aluminum alloys[27]. Meanwhile, unbonded condition in the middle of the cylinder were also encountered in stainless steel welding due to excessively low rotation speeds[10]. All these studies agreed that the defects could be attributed to the unsuitable welding parameters selected. However, no defects were observed in the joints based on the observations of this study.

A closer look at the microstructure reveals more distinct changes in grain size from the interface to the deformation zone. This is illustrated in Fig.8. The figure shows nearly equiaxed austenite grains at the bond interface. The interlayer thickness is approximately 500 µm, as indicated by the scale bar in the figure. The microstructure next to the interface exhibited a darker and thinner layer. This layer is about half as thick as the middle layer. Beyond this layer, a deformed structure is evident. This deformed structure progressed from the interface until it reached the base metal, which was unaffected by the welding process.

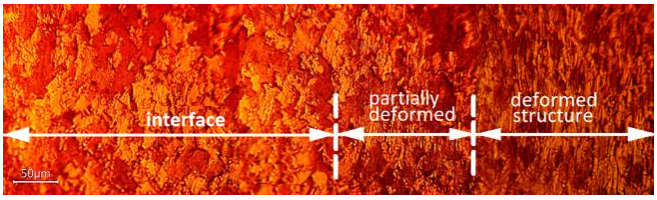

Fig. 8. Gradation of microstructure at the joint.

Fig.9 shows the microstructure in better detail when viewed at a higher magnification (400X). The figure indicates the structure's gradation from the interface towards the deformed structure approaching the base metal. Fig.9(a) depicts the fine, equiaxed grain structure of 304 SS base metal. The structure demonstrates the base metal, which was unaffected by the heat dissipated during

the welding process. Fig.9(b) illustrates the structure at the joint interface. It shows equiaxed grains with a larger size. The deformed structure at the joint is shown in Fig.9(c) and Fig.9(d). The boundary between the interface and the initiation of the deformed structure is seen in Fig.9(c). The signs of the deformed structures are shown in the figure. This part is represented in Fig. 7 by the thin, dark layer between the interface and the deformed structure. This section is referred to as the "partially deformed structure" in this paper since the deformed shape is barely visible.

Fig. 9(d) depicts the structure at the deformed part of the joint. The deformation is clearly visible as an elongated grain. This is the last part of the joint to be affected by the welding process. The deformed zone ended when it reached the unaffected base-metal zone. Deformation at high temperatures caused by friction and forging pressure produces deformed structure. The deformed structure gradually decreased adjacent to the interface, resulting in large, equiaxed grains at the interface. The gradation of the structure indicates the presence of the recrystallization process. The most heat was generated during the welding process at the joint interface. This was then absorbed by the material. The heat dissipation also removed the effect of deformation and reduced the deformed structure, subsequently resulting in a partially deformed structure (Fig.9(c)). The interface structure (Fig.9(b)), like the base metal, is composed of equiaxed grains. However, the grains are coarser than in the base metal structure. RFW generated the most heat at the interface [23], [28]. High heat fluxes at the interface stimulate the recrystallization process. This enabled grain growth, which resulted in coarse grains at the joint interface (Fig.9(b)). A higher heat flux was observed in the RFW of 304 stainless steel, which promoted grain growth [29].

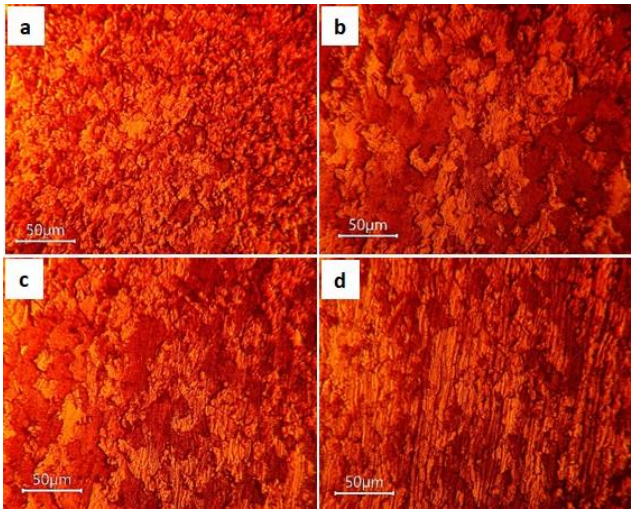

Fig. 9. Microstructure of the joint; (a) base metal, (b) joint interface, (c) partially deformed structure, (d) deformed structure.

3.3 Tensile Strength

All the 24 experimental runs were performed. All 24 experiment runs have been taken. The experimental data are listed in Table 3. The tensile test data were believed to represent the real joint strength since the test was designed to yield maximum stress at the welding joint. In contrast to the mild steel result [4], [5], [6], welding flash for stainless steel friction welding yields regular forms, and it shows that a material with higher hardness produces better welding quality. Even for high friction pressure and time, the yield of the welding flash did not show excessive levels, but it still gave a tidy round shape. Moreover, along with each experiment run that has been conducted, a trend toward bigger welding flash occurred gradually as the friction factor levels increased.

Based on the significance level of 5%, it is shown in Table 4 that the individual and interaction effects are statistically significant. Since the interaction between both factors is significant, the interpretation of influencing factors cannot be individually separated [23]. Thus, this result seems to recommend finding such an optimal level combination between both factors using advanced analysis, e.g., response surface methodology [24].

Table 3. Experiment results from 24 runs

Run	Factors		Fixed setting			Resp.
	P_f (bar)	t_{frc} (s)	P_{forge} (bar)	t_{forge} (sec)	Rev. (RPM)M)	UTS (MPa)
1	5	7				641.251
2	90	11				789.317
3	5	3				67.162
4	55	11				766.708
5	20	11				817.246
6	5	11				786.657
7	55	7				832.540
8	5	3				118.364
9	5	11				781.338
10	20	11				814.586
11	55	11				793.307
12	5	7	100	3	1330	451.513
13	55	7				814.586
14	55	3				851.824
15	90	11				831.875
16	90	3				758.064
17	90	7				826.555
18	20	3				877.093
19	20	7				813.256
20	20	7				798.627
21	90	7				843.180
22	20	3				823.896
23	90	3				856.479
24	55	3				867.118

Table 4. Anova for tensile strength

Source	DF	SS	MS	F	P
Pressure	3	540478	180159	78.99	0.000
Time	2	88320	44160	19.361	0.000
Pressure* time	6	414466	69078	30.29	0.0
Error	12	27369	2281		
Total	23	1070633			

It was noticed that the generated heat at the friction welding joint plays an important role in achieving a joint in RFW. Sufficient heat was required to attain the joint. High heat was thought to push the brittle phase out of the joint when welding dissimilar materials. This avoided brittleness at the joint [17]. However, it has also been suggested that overheating at the interface should be avoided. Hence, friction pressure and friction time should be properly controlled [30].

Theoretically, friction pressure and rotation speed are positively correlated with energy (heat generated) at the interface. The positive impact of rotation speed on heat generation was illustrated by numerical simulation. Conversely, itwas also found that a longer friction time reduction resulted in lower heat generation[5]. This discussion revealed that the relationships between RFW parameters and joint quality were quite complex.

The simultaneous interpretation of both factors in the present work is shown in Fig.10 and Fig. 11. The figure displays the main (Fig.10) and interaction (Fig. 11) effects of the friction pressure and the friction time parameters. For friction pressures above five bars, it is shown that at any friction time setting, different friction pressures do not give variation in tensile strength. It means that, when fixed factors are considered, stainless steel friction welding will provide a strong joint at least at 20 bars with a minimum friction time of three seconds. Adding time or pressure does not always produce the strongest result. In contrast, at a certain point, the tensile strength was reduced.

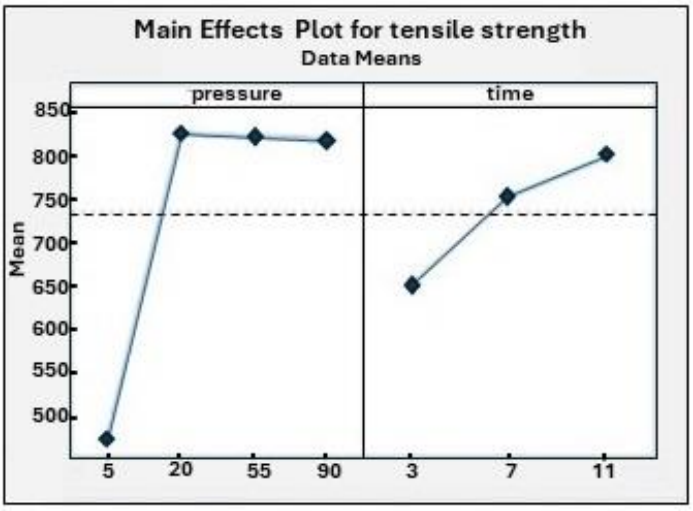

Fig. 10. Main effect plot from both factors.

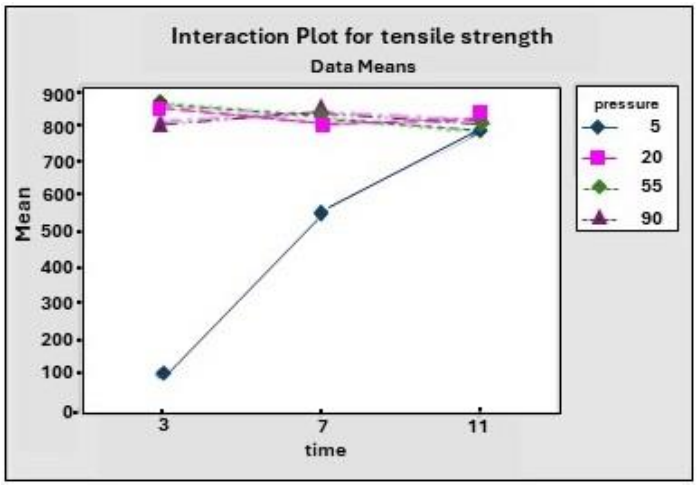

Fig. 11. Interaction effect plot from both factors.

An anomaly occurred at five bars of friction pressure and afriction time of. Increasing the friction times at five bars of friction pressure leads to higher tensile strength as well as higher friction pressure, yet it will not work for any other setting. This point acts as the potential critical level in stainless steel friction welding, and this setting should be avoided even if it still provides a perfect joint. Based on the interpretation of the interacting factors and the anomaly within, it is not recommended to increase each factor individually to obtain a stronger joint. This result is in line with the studies that studied the RFW of stainless steel using the Taguchi DoE approach [9]. These studies have recommended an optimum point for several factors. The suggested optimum condition indicated the interaction of those factors.

There is a potential equilibrium point as both factors will give the highest tensile strength. This point leads to the possibility of an optimal setting for both factors. Adding new, narrower levels for both factors captures the tensile strength variation of the lower levels compared to the higher ones, resulting in the anomaly mentioned. This addition may provide a clearer interaction graph and capture the relationship between both factors in influencing the tensile strength, although it requires additional experimental runs and increases the cost.

3.4 Microhardness Across the Joint

Microhardness tests were carried out across the joint in the longitudinal direction to evaluate the hardness structure at the joint. This was also performed to study the effect of heating and cooling cycles on the hardness of the joint. The hardness profile across the joints is shown in Fig. 12. The hardness of the joint interface and the base metal do not show any difference. However, the two parts near the interface exhibits higher hardness.

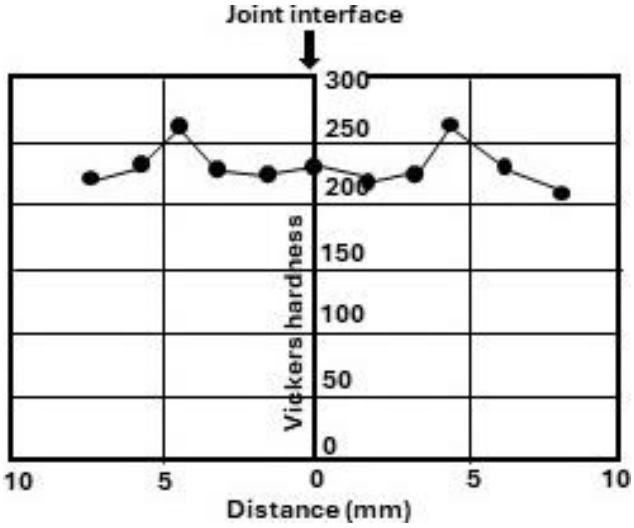

Fig. 12. Variation of hardness across the joint, taken longitudinally at the center of the sample.

The hardness of the structure is influenced by secondary-phase precipitation, grain refinement, and an increase in the dislocation density [31]. RFWs of different materials found that the combination of grain refinement and the formation of secondary phases increased the hardness of the joint [32]. In the present study, the observation of the microstructure did not indicate any phase changes. This may be because the same material was welded. Welding of the same materials did not produce any element diffusion that could initiate secondary phase formation. Furthermore, the rapid cooling occurring in RFW can prevent the formation of intermetallic compound. This is inline with several studies on the RFW of stainless steel (*i.e.*, duplex [31] and 316 [33]) that did not find any intermetallic compound precipitation.

The heat generated during the RFW process dissipated into the material. As the material moved away from the interface, it experienced lower temperatures. The deformation, caused by the friction and forge pressure applied during the process, was revealed by the elongated grain. At lower temperatures, continuous work hardening was observed in the hot deformation of stainless steel [34]. This observation could account for the high hardness of the deformed structure. In the hot deformation of stainless steel, elevated temperatures prevent the activation of the hardening mechanism [34]. Under these conditions, the material undergoes dynamic recovery and recrystallization, hindering work hardening. This phenomenon is particularly notable in the interface joint, which maintains the highest temperature throughout the process.

The coarse grains observed at the interface resulted from recrystallization at higher temperatures and for longer durations. Elevated temperatures and extended periods encourage grain growth, leading to a coarse grain structure [35]. As depicted in Fig. 8, the presence of coarse grains at the interface is correlated with a lower hardness. Coarse grains exhibit lower dislocation density compared to fine grains, facilitating unrestrained dislocation movement and making plastic deformation formation more accessible [36]. Therefore, the presence of coarse grain in the joint interface is likely a contributing factor to its lower hardness.

4 Conclusion

The study conducted on friction welding of 304 stainless steel has revealed that the friction parameters of RFW play a crucial role in achieving a high-quality joint. Increasing the friction pressure has been found to improve joint strength; however, it is important to note that there may be an optimum pressure, as strength tends to decrease at higher pressures (*e.g.*, 90 MPa). The highest recorded tensile strength of the joint (851.824 MPa) was achieved using a friction pressure of 55 bar and friction time of 3

s. The efficiency of RFW, in comparison to the tensile strength of 304 stainless steel, was found to be 103.6%.

The relationship between the friction pressure and time is complex, and optimizing the tensile strength presents challenges. It seemed that a balance could be achieved at approximately 11 s of friction time, indicating the need for a more comprehensive analysis with a wider range of factors. A critical point for stainless steel friction welding was identified at 5 bars of friction pressure and 3 s of friction time, as the parameters below this point resulted in weak strength or incomplete bonding. It is therefore recommended to avoid applying friction pressure below 5 bars in RFW practices involving 304 stainless steel. Interestingly, at a friction pressure of 5 bar, increasing the friction time significantly improved the joint strength; however, extending the friction time did not have an impact on the tensile strength at higher friction pressures.

The microstructure of the joint consisted of three distinct zones: the deformation zone, the partially deformed zone, and the interface joint with coarse equiaxed grains. The presence of coarse grains at the interface was attributed to grain growth during the dynamic recrystallization process, which reduced the hardness at the joint interface. The deformed zone exhibited a strain-hardening effect, as indicated by the elevated hardness, and significantly contributed to the overall tensile strength of the joint. In conclusion, this study provides valuable insights into the complex relationship between parameters in friction welding of 304 stainless steel, highlighting potential areas for optimization and further exploration.

Acknowledgement

The authors express their gratitude to the Ministry of Education, Culture, Research, and Technology, Republic of Indonesia, specifically the Directorate of Research and Community Services, for their support in funding this research under the Multiyear Competitive Fundamental Research scheme, with contract numbers 003/AMDSP2H/ LTMULTI/PDPK/LL7/2021 and 006/SPLit/AMD/ LPPM/01/Dikbudristek/Multi/FT/VII/2021.

References

[1] A. Prastyo, F. Ibrahim, and M. Badaruddin, "Analysis of Mechanical Properties of CD 304 SS at High Temperature Transient Condition," *J. Polimesin*, vol. 20, no. 2, pp. 169–175, 2022, [Online]. Available: https://e-jurnal.pnl.ac.id/polimesin/article/view/2995

[2] K. T. Sunny and N. N. Korra, "A systematic review about welding of super austenitic stainless steel," in *Materials Today: Proceedings*, Elsevier Ltd, 2021, pp. 4378–4381. doi: 10.1016/j.matpr.2021.05.185.

[3] A. R. Hakim and I. Imran, "Analisa pengaruh variasi kampuh terhadap hasil pengelasan SMAW pada stainless steel 304 menggunakan pengujian ultrasonic dan kekuatan tarik," *J. Polimesin*, vol. 18, no. 1, pp. 30–38, 2020.

[4] V. A. Alza, "Mechanical Properties and Microstructure, in welded joints of Low and Medium Carbon Steels, Applying Rotary Friction," *Int. J. Recent Technol. Eng. ISSN*, pp. 2277–3878, 2020.

[5] Y. Yohanes, R. Abdurrahman, and A. Ridwan, "Finite element study on rotary friction welding process for mild steel," in *IOP Conference Series: Materials Science and Engineering*, IOP Publishing, 2019, p. 012111. doi: 10.1088/1757-899X/620/1/012111.

[6] S. T. Selvamani, K. Palanikumar, K. Umanath, and D. Jayaperumal, "Analysis of friction welding parameters on the mechanical metallurgical and chemical properties of AISI 1035 steel joints," *Mater. Des.*, vol. 65, pp. 652–661, 2015.

[7] Y. Lu, D. Li, J. Zhang, C. Bi, F. Sun, and Y. Yang, "Effects of Friction Pressure on Microstructures and Mechanical properties of friction welded Super304H austenitic welding joints," in *IOP Conference Series: Materials Science and Engineering*, IOP Publishing, 2020, p. 012002.

[8] G. Wang, J. Li, W. Wang, J. Xiong, and F. Zhang, "Study on the effect of energy-input on the joint mechanical properties of rotary friction-welding," *Metals (Basel).*, vol. 8, no. 11, p. 908, 2018.

[9] H. Mesmari and F. Krayem, "Mechanical and microstructure properties of 304 stainless steel friction welded Joint," *Int. Res. J. Eng. Sci. Technol. Innov.*, vol. 2, no. 4, pp. 65–74, 2013.

[10] N. Mathiazhagan, T. Senthilkumar, and V. Balasubramanian, "Effect of Mechanical Properties and Microstructural Characteristics of Friction Welded Austenitic Stainless Steel Joints," *Aust. J. Basic Appl. Sci.*, vol. 9, no. 27, pp. 267–276, Aug. 2015, [Online]. Available: www.ajbasweb.com

[11] M. Sahin, "Evaluation of the joint-interface properties of austenitic-stainless steels (AISI 304) joined by friction welding," *Mater. Des.*, vol. 28, no. 7, pp. 2244–2250, 2007.

[12] M. Acarer and B. Demir, "An investigation of mechanical and metallurgical properties of explosive welded aluminum-dual phase steel," *Mater. Lett.*, vol. 62, no. 25, pp. 4158–4160, May 2008, doi: 10.1016/j.matlet.2008.05.060.

[13] M. Mohanta, S. Kar, D. Mohanta, and A. M. Mohanty, "Experimental Analysis and Parametric Optimization of 6065-Aluminium Alloy in Rotary Friction Welding," *Int. J. Adv. Mech. Eng.*, vol. 8, no. 1, pp. 111–118, 2018, [Online]. Available: http://www.ripublication.com

[14] F. Khalfallah, Z. Boumerzoug, S. Rajakumar, and E. Raouache, "Optimization by RSM on rotary friction welding of AA1100 aluminum alloy and mild steel," *Int. Rev. Appl. Sci. Eng.*, 2020.

[15] Y. Chapke, D. Kamble, and S. M. S. Shaikh, "Friction welding of Aluminium Alloy 6063 with copper," in *E3S web of conferences*, EDP Sciences, 2020, p. 02004.

[16] A. Handa and V. Chawla, "Investigation of mechanical properties of friction-welded AISI 304 with AISI 1021 dissimilar steels," *Int. J. Adv. Manuf. Technol.*, vol. 75, pp. 1493–1500, 2014.

[17] Y. Belkahla *et al.*, "Rotary friction welded C45 to 16NiCr6 steel rods: statistical optimization coupled to mechanical and microstructure approaches," *Int. J. Adv. Manuf. Technol.*, vol. 116, pp. 2285–2298, 2021.

[18] Z. Yanushkevich, A. Lugovskaya, A. Belyakov, and R. Kaibyshev, "No Title," *Mater. Sci. Eng. A*, vol. 667, pp. 279–285, 2016, [Online]. Available: https://www.sciencedirect.com/science/article/abs/pii/S0921509316305019

[19] G. E. P. Box, J. S. Hunter, and W. G. Hunter, "Statistics for experimenters," in *Wiley series in probability and statistics*, Wiley Hoboken, NJ, 2005.

[20] H. Firmanto, S. Candra, M. A. Hadiyat, and Y. Haryono, "Influence of Heating Stage Parameters on the Joint Strength of Rotary Friction Welded AISI 1045 and AISI 304 Steels: A Polynomial Model," in *Materials Science Forum*, Trans Tech Publ, 2022, pp. 157–163.

[21] A. Vairis and M. Petousis, "Designing experiments to study welding processes: using the Taguchi method," *J. Eng. Sci. Technol. Rev.*, vol. 2, no. 1, pp. 99–103, 2009.

[22] V. Olden, Z. L. Zhang, E. Østby, B. Nyhus, and C. Thaulow, "Notch tensile testing of high strength steel weldments," in *2nd international symposium on high strength steel*, 2002.

[23] E. P. Alves, R. C. Toledo, F. Piorino Neto, F. G. Botter, and C. Ying An, "Experimental thermal analysis in rotary friction welding of dissimilar materials," *J. Aerosp. Technol. Manag.*, vol. 11, p. e4019, 2019.

[24] M. Gavalec, I. Barényi, and H. Chochlíková, “Properties and microstructure of joints created by the method of rotary friction welding,” in *Proceedings 31st International Conference on Metallurgy and Materials*, Brno, 2022, pp. 376–381. doi: https://doi.org/10.37904/metal.2022.4406.
[25] M. Gavalec, I. Barenyi, M. Krbata, M. Kohutiar, S. Balos, and M. Pecanac, “The effect of rotary friction welding conditions on the microstructure and mechanical properties of Ti6Al4V titanium alloy welds,” *Materials (Basel).*, vol. 16, no. 19, 2023, doi: https://doi.org/10.3390/ma16196492.
[26] M. C. Zulu and P. M. Mashinini, “Analysis of defect formation during rotary friction welding of titanium alloy,” in *Proceedings of 2021 IEEE 12th International Conference on Mechanical and Intelligent Manufacturing Technologies, ICMIMT 2021*, 2021, pp. 7–11. doi: 10.1109/ICMIMT52186.2021.9476169.
[27] A. Sasmito, A. S. Hermawan, and Sunyoto, “Rotary friction welding properties of AA5083-H112/AA7075-T6 joints: Parameter and low temperature effect,” *Mater. Sci. Technol.*, 2024, doi: https://doi.org/10.1177/02670836241234198.
[28] A. B. Dawood, S. I. Butt, G. Hussain, M. A. Siddiqui, A. Maqsood, and F. Zhang, “Thermal model of rotary friction welding for similar and dissimilar metals,” *Metals (Basel).*, vol. 7, no. 6, p. 224, 2017.
[29] G. L. Wang, J. L. Li, J. T. Xiong, P. Y. Ma, W. L. Wang, and F. S. Zhang, “A heat flux model for rotary friction welding of 304 stainless steel,” *Mater. Res. Express*, vol. 6, no. 2, p. 026558, 2018.
[30] P. Gaikwad, S. Naik, N. Dhutre, S. Maniyar, and V. Kulkarni, “Parametric Analysis of Rotary Friction Welding Process Based On Comparative Study between Mild Steel and Stainless Steel 304,” *Int. J. Res. Eng. Appl. Manag.*, vol. 5, no. special issue, pp. 224–228, 2019.
[31] S. Zhang, F. Xie, X. Wu, J. Luo, W. Li, and X. Yan, “The Microstructure Evolution and Mechanical Properties of Rotary Friction Welded Duplex Stainless Steel Pipe,” *Materials (Basel).*, vol. 16, no. 9, 2023, doi: 10.3390/ma16093569.
[32] A. M. Mahajan, N. K. Babu, M. K. Talari, A. U. Rehman, and P. Srirangam, “Effect of Heat Treatment on the Microstructure and Mechanical Properties of Rotary Friction Welded AA7075 and AA5083 Dissimilar Joint,” *Materials (Basel).*, vol. 16, no. 6, 2023, doi: 10.3390/ma16062464.
[33] A. J. Hassan, B. Cheniti, B. Belkessa, T. Boukharouba, D. Miroud, and N. E. Titouche, “Metallurgical Investigation of Direct Drive Friction Welded Joint for Austenitic Stainless Steel,” *Acta Metall. Slovaca*, vol. 29, no. 2, pp. 88–92, Jun. 2023, doi: 10.36547/ams.29.2.1802.
[34] A. Dehghan-Manshadi, M. R. Barnett, and P. D. Hodgson, “Recrystallization in AISI 304 austenitic stainless steel during and after hot deformation,” *Mater. Sci. Eng. A*, vol. 485, no. 1–2, pp. 664–672, 2008.
[35] M. S. Anwar, R. R. Widjaya, L. B. A. Prasetya, A. A. Arfi, E. Mabruri, and E. S. Siradj, “Effect of Grain Size on Mechanical and Creep Rupture Properties of 253 MA Austenitic Stainless Steel,” *Metals (Basel).*, vol. 12, no. 5, p. 820, 2022.
[36] R. Ke, C. Hu, M. Zhong, X. Wan, and K. Wu, “Grain refinement strengthening mechanism of an austenitic stainless steel: Critically analyze the impacts of grain interior and grain boundary,” *J. Mater. Res. Technol.*, vol. 17, pp. 2999–3012, 2022.